

Performance and wake conditions of a rotor located in the wake of an obstacle

I V Naumov¹, I K Kabardin¹, R F Mikkelsen², V L Okulov^{1,2}, J N Sørensen²

¹Kutateladze Institute of Thermophysics, SB RAS, Novosibirsk 630090, Russia

²Department of Wind Energy, Technical University of Denmark, 2800 Lyngby, Denmark

E-mail: naumov@itp.nsc.ru

Abstract. Obstacles like forests, ridges and hills can strongly affect the velocity profile in front of a wind turbine rotor. The present work aims at quantifying the influence of nearby located obstacles on the performance and wake characteristics of a downstream located wind turbine. Here the influence of an obstacle in the form of a cylindrical disk was investigated experimentally in a water flume. A model of a three-bladed rotor, designed using Glauert's optimum theory at a tip speed ratio $\lambda = 5$, was placed in the wake of a disk with a diameter close to the one of the rotor. The distance from the disk to the rotor was changed from 4 to 8 rotor diameters, with the vertical distance from the rotor axis varied 0.5 and 1 rotor diameters. The associated turbulent intensity of the incoming flow to the rotor changed 3 to 16% due to the influence of the disk wake. In the experiment, thrust characteristics and associated pulsations as a function of the incoming flow structures were measured by strain gauges. The flow condition in front of the rotor was measured with high temporal accuracy using LDA and power coefficients were determined as function of tip speed ratio for different obstacle positions. Furthermore, PIV measurements were carried out to study the development of the mean velocity deficit profiles of the wake behind the wind turbine model under the influence of the wake generated by the obstacle. By use of regression techniques to fit the velocity profiles it was possible to determine velocity deficits and estimate length scales of the wake attenuation.

1. Introduction

Wind turbines are often sited near obstacles such as forests, ridges, hills and cliffs [1]. These obstacles can strongly disturb the wind velocity profile [2]. Some of them can be very favorable for producing wind power, whereas others should be avoided, as they may generate considerable flow stagnation ("wind shadow") in the rotor area (fig. 1). It is critical to identify both positive and negative effects to be able to predict the overall performance of a wind turbine. The effects of the different obstacles on the energy production and turbine loading are not fully understood and the development of the wake of a wind turbine operating behind obstacles is still not well understood [3]. The aim of the present investigation is to elucidate these effects.

An obvious negative factor decreasing the turbine efficiency is the generation of a velocity deficit or "wind shadow" in front of the rotor. Thus, a selection of the turbine location relative to the obstacle is an important issue. The factors affecting "wind shadows" are wind turbine hub height, separation distance, roughness length, roughness class, obstacle height, etc. An ideal place is a smooth hilltop



with the absolutely flat open area around it. But such locations are rarely found. In most cases it is required to install wind turbines at relatively large distances from obstacles or to place the wind turbine rotor above obstacles.

Another issue is that the obstacles appearing in front of wind turbine rotors increase the turbulence level. The turbine efficiency depends on the nature of the turbulence. Increasing the level of free-stream turbulence may lead to an earlier breakdown of the vortex wake behind the wind turbine, which may be of importance for the design of wind farms [4]. The impact on wind turbine efficiency due to large-scale coherent turbulent structures formed by an obstacle in front of a wind turbine was studied in [5]. In their laboratory experiment, a model of a hydrokinetic turbine was examined to study the influence of coherent structures on power pulsations and wake development. The turbine model was placed in a channel with an open-flow and operated under subcritical conditions. The incoming flow was perturbed by vertically oriented cylinders of various diameters. It cylinder array was established such that the coherent structures generated by the cylinders most effectively broke the helical tip vortices. Among other things, it was found that the velocity deficit in the wake 10 diameters downstream of the rotor became lower than it is in the flow without the cylindrical obstacles.

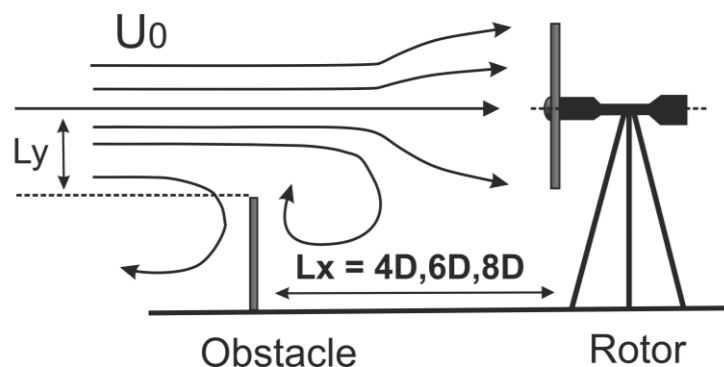


Figure 1. Sketch of the problem.

The purpose of the present work is to study the influence of large-scale obstacles on rotor performance and turbulence levels. As a first case, which also has been investigated by others, we have chosen the simple case of a circular disk. It should be mentioned that recent results for a rotor model in a free flow have shown two interesting properties of the wake behavior: a decreasing velocity deficit following a power law of $-2/3$ in the wake [6] and strong oscillations with a frequency corresponding to the Strouhal number [7]. In the present paper, we use a disk of diameter $0.9D$ as a simplification of a real obstacle and to be in accordance with earlier studies on disk wakes [8]. The disk was axially placed at different positions $L_x = 4D$, $6D$ and $8D$ in front of the rotor (fig.2). In the some tests, the disk was placed at a fixed distance of 6 diameters upstream of the rotor, with the disk axis placed at an vertical offset from the rotor axis of $L_y = 0.5D$ and $1D$, respectively, (fig.2). The experiment took place in the same water flume as used in previous experiments [5-8] to provide a correct comparison and to have the capability of performing additional visualizations. It should be emphasized that for the present setup with Reynolds numbers in the range $140.000 < Re < 240.000$, there are no fundamental differences between performing the experiments in water or in air [8].

At first, employing Laser Doppler Anemometry (LDA), we examined the structure and oscillations of the flow disturbances emanating from the disk to the rotor. Next, the influence of the disk wake on the rotor performance and thrust characteristics were studied at the different disk positions (L_x and L_y). Finally, Particle Image Velocimetry (PIV) experiments were carried out to study the development of the wake behind the rotor, with the rotor placed at the different positions in the disk wake. Non-axisymmetric disturbances by a disk on the semi-similarity of the rotor wake were previously studied [6] at different cross-sections downstream of the rotor and for different tip speed ratios. For comparison, some of these results will also be shown in the following.

2. Experimental Method and Results

The experiments were carried out in a water flume (fig. 2). The length of the flume is 35m, the width is 3m, and the height is 1.0 m, with 3 m transparent walls in the test section. A detailed description of the water flume can be found in [6, 7]. The initial flow in the flume was subject to a very low turbulence level with a uniform velocity profile limiting the influence of external disturbances in the experiments. As mentioned above, a disk with a diameter close to the one of the rotor was used as obstacle. The properties of the wake behind a single disk are well described from previous experiments [8]. A three-bladed model rotor was positioned downstream of the disk. The rotor has a diameter $D = 2R = 0.376\text{m}$, and the blades, consisting of SD7003 airfoil sections, were specially designed for optimum operating conditions at a tip speed ratio $\lambda = 5$ [6, 7], where $\lambda = \Omega R/U$, and Ω is the angular speed of the rotor. The distance from the disk to the rotor changed from $L_x = 4D$ to $8D$ with vertical offsets from the rotor axis of $L_y = 0, 0.5D$ and $1D$, respectively. The Reynolds number, which is based on rotor diameter and the initial flow in the flume, varies in the range $140.000 < Re < 240.000$. There is a weak sensitivity on the behavior of the helical vortices in the wake for these Reynolds numbers. The study of Chamorro et al. [9] suggest that main flow statistics become independent when $Re \geq 93.000$, which are lower than the value used in the current experiments.

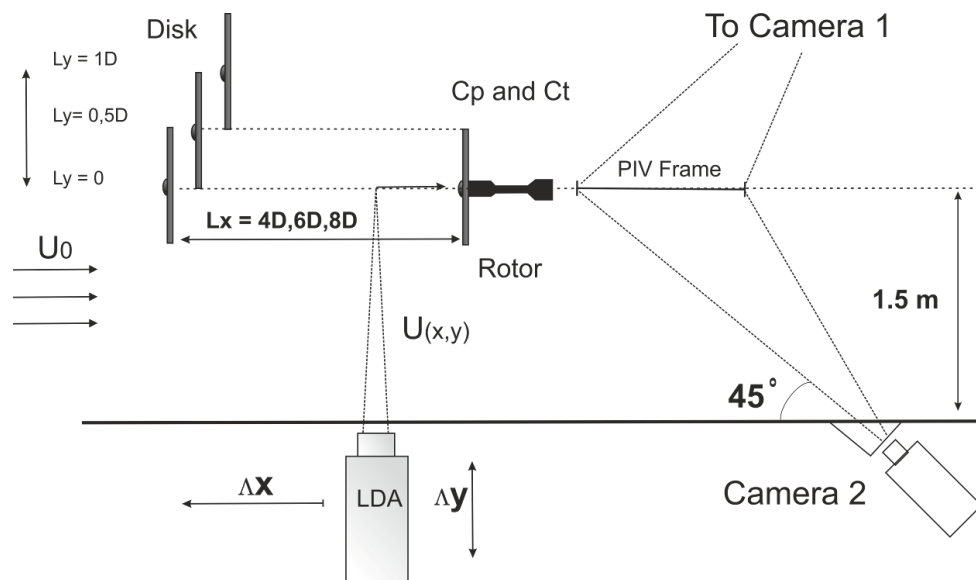


Figure 2. A sketch of the experimental setup.

At first, the incoming flow velocity to the rotor was measured with high temporal accuracy using LDA. The initial free flow in the setup area of the flume has a uniform velocity profile with velocity $U_0 = 0.54 \text{ m/s}$ and turbulence level 3 % [7]. The current measurements were carried out to determine the velocity profile upstream of the rotor subject to the influence of the wake from the disk. The local history of the axial velocity in each point was obtained using a Dantec 2-D Fiber flow LDA, based on a 1W Argon laser with a differential optical configuration and a frequency shift of 40 MHz. The diameter of the optical gauge is 112 mm and the focal length is 600 mm, with a beam diameter of 1.35 mm. The wavelength of the laser beam is 514.5 nm (green light). The size of the probing optical field was $0.12 \times 0.12 \times 1.52 \text{ mm}^3$.

These LDA measurements of both velocity deficit and velocity oscillations (RMS) are shown in figs. 3a and 3b, respectively. The velocity profiles were measured at distance of $0.5D$ upstream of the rotor. The velocity profile reduces with 20 % and the velocity oscillations increases with up to 14% when the disk and rotor placed on a common axis ($L_y = 0$). Increasing L_y , the velocity deficit in the rotor axis decreases only 0.87 % when $L_y = 0.5D$, and at $L_y = 1D$ the velocity deficit almost disappears

in the rotor area (fig. 3a). The LDA measurements show that the level of RMS varies in range from 3 to 16 % and becomes close to the turbulence intensity of the free flow when $L_y=1D$ (fig. 3b).

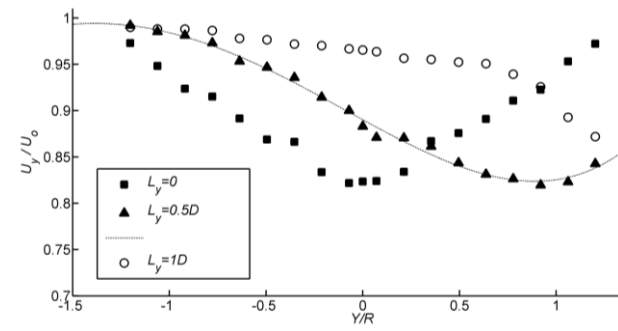


Figure 3a. LDA velocity profiles at $L_x=6D$.

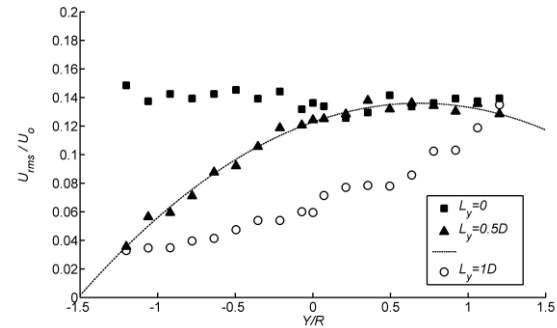


Figure 3b. LDA velocity pulsation at $L_x=6D$.

As a second step, the influence of the obstacle on rotor performance and thrust was examined. The power and thrust coefficients, C_P and C_T , were measured for different tip speed ratios (fig. 4 a, b) by strain gauges, which were mounted in the rotor. The electric signal from the strain gauge sensors was recorded with a frequency of 100 Hz in an interval of 60 s. In total 6000 counts were performed. A FFT plot of one of the samples is shown in fig. 4 c. The existence of a strong peak for all spectra of the C_T signal reveals the existence of a strong frequency of 0.27 Hz in the disk wake, corresponding to the Strouhal [7]. Fig. 4.d shows that the RMS values of C_T decrease when increasing L_y . A similar behavior of these characteristics was also found at distances $L_x=4D$ and $L_x=8D$.

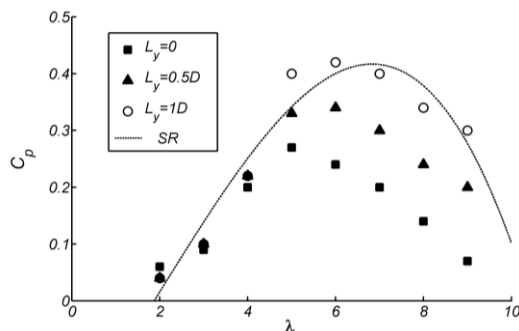


Figure 4a. Power coefficients C_P at $L_x=6D$.

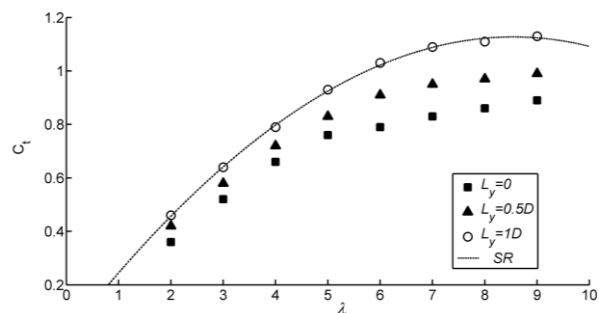


Figure 4b. Thrust coefficients C_T at $L_x=6D$.

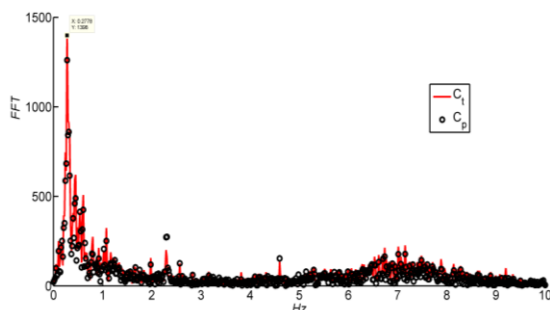


Figure 4c. Spectra of C_T signal at $L_x=6 D$, $\lambda=5$.

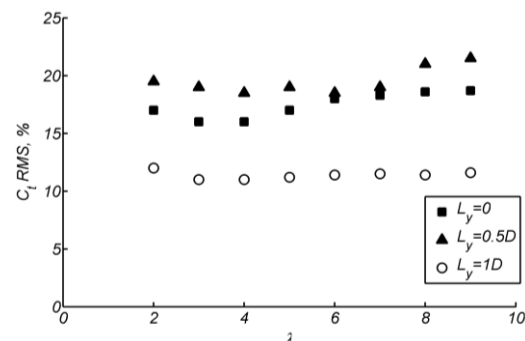


Figure 4d. RMS values of C_T signal at $L_x=6D$.

The more detailed dependences on the power coefficients for different values of L_x and L_y are shown in figure 5. The experimental data for a single rotor without the disk-obstacle is in the figure shown by the solid line.

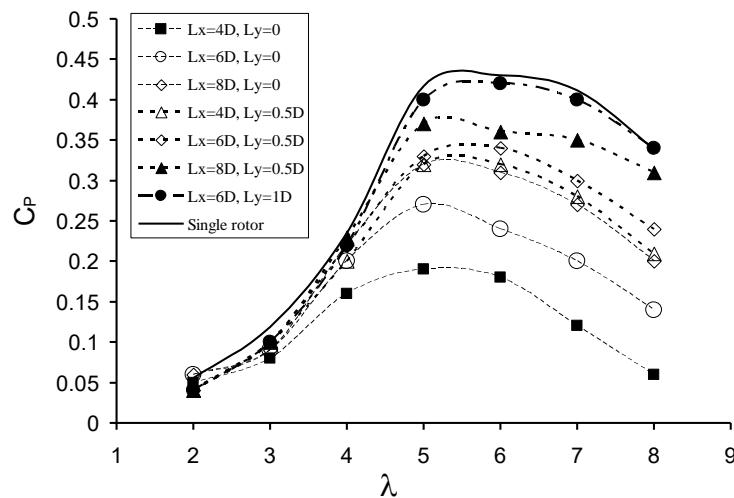


Figure 5. Power coefficients C_p for different values of L_x and L_y .

These dependences show that the wake behind the disk has a strong influence on the rotor performance when the rotor axis coincides with the disk axis ($L_y = 0$). In general, the impact of the disk wake decreases when decreasing L_x . As seen on the plot, the disk wake has nearly no influence on the rotor performance when $L_y = 1D$. The power coefficients in the last case nearly equalled the one of a single rotor without disk-obstacle (solid curve).

3. Development of the rotor wake

The maximum velocity deficit of the wake behind the rotor operating at $\lambda = 5$ was measured for different values of L_x and L_y . PIV experiments were carried out to study the development of mean velocity profiles in the wake downstream of the wind turbine model. In the PIV experiments the Dantec stereo PIV system was used to determine two velocity components in a light sheet vertically crossing through the rotor axis. The light source was a Nd:YAG laser producing 120mJ of energy in a single pulse at a wavelength of 532 nm and an operating frequency of 15Hz. The images were recorded by two Dantec HiSense II cameras with 1344x1024 pixels resolution. Based on the recorded images, the 3-D velocity field was calculated using Dantec Dynamic Studio 2.21 software. The PIV measuring area was 0.22 x 0.35m. Both cameras were placed perpendicularly to each other on the different sides of the flume at angle of 45° to the walls (figure 2). Water-filled optical prisms were installed between the cameras and the walls of the test section to reduce the distortions of the camera inclination to the walls. The focus plane was adjusted using Scheimpflug adapters because the cameras were placed at different angles to the light sheet (see fig. 2).

Various empirical approaches have been applied to describe wind turbine wakes. Recently, a suitable general model for the rotor wakes was determined by analysing the far wake development behind axisymmetric bluff bodies [6, 10-11]. Indeed the common axisymmetric solution to fit the wake behaviour behind a bluff body at high Reynolds was thoroughly tested by a comparison with experimental data for the wake behind a streamline disk in a wind tunnel [12-13]. This theory for the circular disk was also confirmed in the water flume [8]. The maximum deficit of the streamwise velocity in the rotor wake for high-Reynolds-number can be described by the same formula,

$$G(x) = \frac{\Delta U(x)}{U_0} = a(x - x_0)^{-\frac{2}{3}} \quad (1)$$

where U_0 is the incoming free velocity, $\Delta U(x)$ is the maximal velocity deficit at location x on the wake axis, and the parameters a and x_0 depend on the type of bluff body or rotor generating the wake. It

should be emphasized, however, that the power $-2/3$ is general and valid for all kinds of bodies and rotors generating a wake. It was found in [6] that the constants $a=0.85$ and $x_0=3.2$ gives an excellent fit of the velocity deficit in the wake downstream of a single rotor.

We also tried to use the formula (1) for the rotor wake disturbed by the disk-obstacle. Figures 6.a and 6.b show the maximum velocity deficit in the wake of the rotor operating at an optimal tip speed ratio as function of different positions (L_x and L_y) of the disk-obstacle. Here, the symbols shows the experimental data obtained from PIV-averaged velocity fields and lines present approximate curves (1).

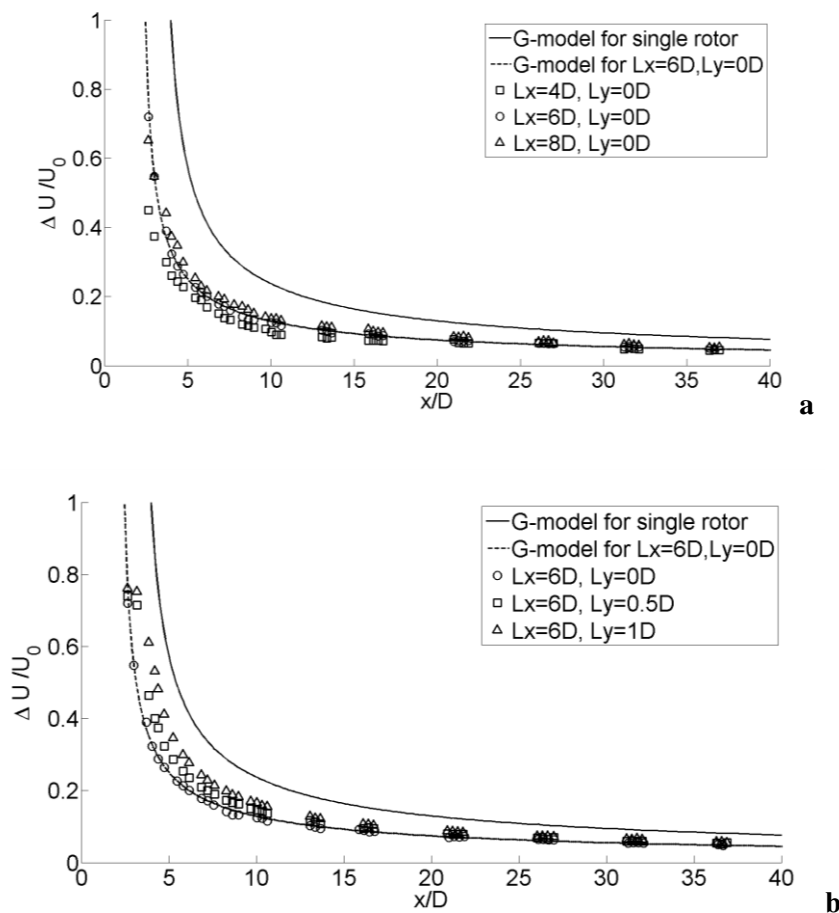


Figure 6. Velocity deficit variation at $\lambda=5$: **a** - different L_x for $L_y=0$, **b** - different L_y for $L_x=6$.

All experimental data monotonically and smoothly decrease by a rate of $-2/3$ in accordance with (1) for the different positions between the disk-obstacle and the rotor. The empirical coefficients, however, still need to be determined. For the common axis ($L_y=0$) at the different distances ($L_x = 4D$, $6D$ or $8D$) the experimental data in figure 6.a look very similar and close to each other. From a simple curve fit, they were approximately found to be $a = 0.51$ and $x_0 = 2.1$. The coefficients in (1) for the disk and rotor arrangement at $L_x = 6D$, $L_y=0.5D$ in figure 6.b are found to be $a= 0.55$, $x_0= 2.55$. For the case of $L_x = 6D$, $L_y = 1D$ the values increase slightly to $a= 0.6$ and $x_0= 3.0$, tending to the values of the wake development for a single rotor without a disk-obstacle. The last curve (without the disk) is higher as those of a rotor operating in the wake behind an obstacle. This is the case even when $L_y = 1D$ or when the disk-obstacle is placed outside the rotor area (figure 2). Here C_p attains approximately the same value as for a single rotor (figure 5). In this case the turbulent oscillations from the obstacle can reduce the velocity deficit of the rotor wake, whereas both the high turbulence level and the “wind shadow” dominate when $L_y = 0$ or $0.5D$.

4. Conclusions

The interaction between a wind turbine rotor and an upstream located obstacle was experimentally studied to estimate the influence of “wind shadow” and flow turbulence on the behaviour of the rotor and resulting wake. The experiments were performed in a water flume subject to a very low turbulence level and a uniform velocity profile, limiting the influence of external disturbances on the disk-rotor flow. LDA measurements showed that the velocity deficit under the influence of the disk may increase with up to 20 % and that the turbulence intensity (RMS value) may increase in the range from 8 to 15 % in a cross-section located in front of the rotor. The dependency on power and thrust coefficients resulting from operating the turbine at different tip speed ratios and disk positions were investigated, and the performance was found to depend strongly on the position of the upstream located disk. Another issue concerned the wake development. Here it was found the power law previously determined for wakes behind single rotors and single disks in general is valid also for interacting wakes behind disks and rotors.

Acknowledgments

The research was supported by the Russian Science Foundation (Project № 14-19-00487) and by the Danish Council for Strategic Research for the project Center for Computational Wind Turbine Aerodynamics and Atmospheric Turbulence (grant 2104-09-067216/DSF) (COMWIND: <http://www.comwind.org>).

References

- [1] Thomas A. Wind Power in Power systems. *John Wiley and sons, ltd.* 2005:1120.
- [2] Sogachev A. Wind energy availability above gaps in a forest. *Proc. 2009 European Wind Energy Conference and Exhibition.* 2009; 6: 4198-4206.
- [3] Vermeer L, Sørensen J, Crespo A. Wind turbine wake aerodynamics. *Prog Aerosp Sci.* 2003; 39: 467-510.
- [4] Porté-Agel F, Wu YT, Chen CH. A numerical study of the effects of wind direction on turbine wakes and power losses in a large wind farm. *Energies.* 2013;6(10): 5297–5313.
- [5] Chamorro LP, Hill C, Neary VS, Gunawan B, Arndt REA, Sotiropoulos F. Effects of energetic coherent motions on the power and wake of an axial-flow turbine. *Physics of Fluids* 2015; 27(5): 055104.
- [6] Okulov VL, Naumov IV, Mikkelsen RF, Sørensen JN. Wake effect on a uniform flow behind wind-turbine model. *J. of Physics: Conference series.* 2015; 625: 012011.
- [7] Okulov VL, Naumov IV, Mikkelsen RF, Kabardin IK, Sørensen JN. A regular Strouhal number for large-scale instability in the far wake of a rotor. *J. Fluid Mech.* 2014; 747: 369-380.
- [8] Naumov IV, Litvinov IV, Mikkelsen RF, Okulov VL. Investigation of a wake decay behind a circular disk in a hydro channel at high Reynolds numbers. *Thermophysics and Aeromechanics* 2015; 22(6): 657-665.
- [9] Chamorro LP, Arndt REA, Sotiropoulos F. Reynolds number dependence of turbulence statistics in the wake of wind turbines. *Wind Energy* 2012; 15: 733–742.
- [10] Dufresne NP, Wosnik M. Velocity Deficit and Swirl in the Turbulent Wake of a Wind Turbine. *J. Marine Technology Society* 2013; 47(4): 193-205.
- [11] Naumov IV, Mikkelsen RF, Okulov VL. Estimation of Wake Propagation behind the Rotors of Wind-Powered Generators. *Thermal Engineering* 2016; 63(3): 208–213.
- [12] George WK. The self-preservation of turbulent flows and its relation to initial conditions and coherent structures. *Advances in Turbulence*, 1989: p. 39-73.
- [13] Johansson PBV, George WK, Gourlay MJ. Equilibrium similarity, effects of initial conditions and local Reynolds number on the axisymmetric wake. *Physics of Fluids*, 2003; 15(3): 603-617.